

# ***Interactive comment on “Opposite Long-term Trends in Aerosols between Lower and Higher Altitudes: A Testimony to the Aerosol-PBL Feedback” by Zipeng Dong et al.***

**Zipeng Dong et al.**

dzp2003@126.com

Received and published: 20 March 2017

## 1. Discussion on the influences of biomass burning aerosols in the atmosphere

Fossil fuel combustion and biomass burning are the main sources releasing carbon aerosols into the atmosphere. Similar to industrial pollution, carbonaceous aerosols emitted from biomass burning, which are characterized by large amount of fine mode particles and comparatively low single scattering albedo, contributes significantly to the earth's radiation balance, consequently changing the atmospheric thermodynamic stability, and thereby cloud formation. As a large agricultural country, China has the highest straw residues yield in the world. Huge amount of corn stovers and wheat straws were burned to clear land during the harvest season every year. The combina-

tion of pollutants from biomass burning and the industrial emissions in China results in regional heavy pollution (Ding et al., 2013). Here, the contribution of biomass burning to carbonaceous aerosols over Guanzhong plain was discussed by employing the aerosol optical depth and fire hot spot data derived from MODIS and the attenuation coefficients acquired by Aethalometer (Model AE-31).

Figure 1 shows the spatial distribution of daytime fire counts in summer during 2002–2014 over mainland China based on AQUA/MODIS collection 6 active fire product. Clearly, the most intense biomass burning activity was detected in Henan, Anhui, Jiangsu, Shandong and Hebei provinces. The open agricultural fires occurred in Guanzhong Plain were much less intense than aforementioned provinces. However, the highest summertime elemental carbon (EC) and organic carbon (OC) concentrations were observed in Xi'an and Chongqing among 14 of China's large cities (Cao et al., 2012), suggesting that the biomass burning is not the main source of carbonaceous aerosols over Guanzhong Plain.

AOD values at 550 nm were regressed against the fire counts over the study region (Fig.2). The result showed the biomass burning activities have an insignificant positive impact on the AOD ( $p=0.25$ ), consistent with that reported by L. Wang et al. (2015).

To further explore the major source of the carbonaceous aerosols in Guanzhong plain, the spectral values of absorption coefficients are estimated base on the attenuation coefficients acquired by Aethalometer (Model AE-31) at Xi'an site ( $108.97^{\circ}\text{E}$ ,  $34.43^{\circ}\text{N}$ , located at northern suburb of Xi'an, belonging to the China Atmosphere Watch Network (Y. Wang et al., 2015)) following the method proposed by Aruna et al. (2013). The spectral dependence of the absorption coefficients of carbonaceous aerosols, namely, the light absorption wavelength exponent ( $\alpha$ ), crucially depends on the source of the aerosols (Aruna et al., 2013; Weingartner et al., 2003). The value of  $\alpha$  can be determined by fitting a power law to the absorption coefficients data:  $\sigma_{\lambda}=\beta\lambda^{(-\alpha)}$ , where  $\sigma_{\lambda}$  is the spectrally dependent absorption coefficients,  $\beta$  is a constant, and  $\lambda$  is the light wavelength.

[Printer-friendly version](#)

[Discussion paper](#)



Numerous studies showed the value of  $\alpha$  is below or close to 1.0 for aerosols from fossil fuel combustion, between 1.5 and 3 for biomass burning aerosols, and between 2 and 3 for dust particles (Sotogarcía, et al., 2011; Aruna et al., 2013 and references therein). As shown in Fig.3, the value of  $\alpha$  derived from the AE-31 at Xi'an is 0.82 and 0.86 in summer of 2011 and 2012, respectively, indicating that the substantial black carbon at Xi'an is predominantly from fossil fuel. It is noted that the  $\alpha$  in wintertime (the value is 1.15) at Xi'an is much higher than that in summertime, which can be explained by abundant domestic biomass combustion for residential heating in winter (Cao et al., 2012; Huang et al., 2014). Moreover, the seasonal EC mass concentration observed by the AE-31 is 8.12 and 6.17  $\mu\text{gm}^{-3}$  in summer of 2011 and 2012, respectively. These results are in good agreement with that reported by Cao et al. (2012).

Overall, the results demonstrate that the biomass burning aerosols over Guanzhong have an insignificant influence on both the concentration of BC and the total column aerosol optical depth in summer.

## 2. More discussion on the PBL dynamics

Absorbing aerosols reduce the net shortwave radiation at the surface and thus lead to a surface cooling. Concurrently, the absorbing particles heat the air at upper levels due to absorption of solar radiation. Hence, they alter the vertical temperature structure, atmospheric stability and large-scale convection. More specifically, absorbing aerosol tended to depress the development of PBL due to a combination of two mechanisms:

Firstly, through scattering and absorption of solar radiation, the absorbing aerosols can induce net surface shortwave radiation (NSSR) reduction and surface cooling. The decreased NSSR is mostly balanced by reduction of sensible heat flux, and only secondarily by decreases in latent heat flux and infrared radiation (Zhang et al., 2008). This will cause the weakening of the turbulent flux of sensible heat transfer into the atmosphere as well as surface buoyancy fluxes (Tesfaye et al, 2014). As a result, the radiative effects of absorbing aerosols can suppress convection processes and induce

[Printer-friendly version](#)

[Discussion paper](#)



a reduction in PBL height.

The aerosol direct radiative forcing was widely reported across China (Li et al., 2010). According to Xia et al. (2007a), instantaneous global shortwave radiation (SWR) at the surface can be parameterized as a function of solar zenith angle (SZA) and AOD:  $F(\theta)=a_1 \times \mu^{\hat{a}_2} \times \exp(a_3 \times \mu^{\hat{a}_4} \times AOD)$ , where  $\mu$  represents the cosine of the SZA,  $a_1$ ,  $a_2$ ,  $a_3$  and  $a_4$  are four parameters relevant to the aerosol optical properties. The instantaneous aerosol direct radiative forcing (ADRF) can then be computed as follows:  $ADRF\_int=(1-\alpha) \times a_1 \times \mu^{\hat{a}_2} \times (\exp(a_3 \times \mu^{\hat{a}_4} \times AOD)-1)$ , where  $\alpha$  represents the surface albedo. In this case, the diurnal ADRF could be finally derived through the 24-h integration of instantaneous ADRF.

The ADRF at Changan site is obtained following the procedure described above by using the AOD retrieved from MFRSR, the MODIS surface albedo products (MCD43B3), as well as the global shortwave radiation and solar direct radiation measured by Kipp-Zonen CMP21 and Eppley Normal Incidence Pyrheliometer (NIP), respectively. The period of the data used is from June 2013 to August 2014. The seasonal mean diurnal ADRF at the surface is -35.7 Wm<sup>-2</sup> for global SWR in summer at Changan. The normalized diurnal ADRF (diurnal ADRF per unit AOD) is -55.1 Wm<sup>-2</sup>. This value is close to that estimated in northern China where the value is -55.2 Wm<sup>-2</sup> (Xia et al., 2007b) and larger than that computed in Taihu where the value is -51.4 Wm<sup>-2</sup> (Xia et al., 2007a), suggesting the single scattering albedo in northern China is much lower. The seasonal mean diurnal variation of the instantaneous ADRF at Changan is shown in Fig.4. The averaged instantaneous ADRF during the daytime showed very large negative values, indicating significant surface cooling and subsequently reduction of sensitive heating flux and PBL height.

Secondly, black carbon aerosols efficiently absorb radiation in the visible wavelengths, trapping the incident solar radiation and consequently warming the atmosphere by a conversion of the incident light into thermal energy. The changes in atmospheric radiative heating rate and thermodynamic structure of the atmosphere induced by those



thermal energy perturbations were highly reliant on vertical location of aerosols. The impact of aerosol heat absorption on convective PBL dynamics for different vertical profiles of aerosol was discussed by Barbaro et al. (2013). In cases of absorbing aerosol located above the boundary layer, the boundary layer suffers a radiative cooling (Johnson et al., 2004). While the absorbing aerosols are present at the top of the PBL, the vertical motions throughout the PBL are reduced and a deeper inversion layer occurs below the entrainment zone as a result of the heat absorption, inducing a much shallower PBL than the case in which the aerosols are uniformly distributed (Barbaro et al., 2013). Overall, in addition to the optical properties of the aerosols, the vertical distribution is an important characteristic determining the influence of aerosol on PBL height evolution. As shown in Fig.5a-b in the original manuscript, the aerosols over Guanzhong are mainly confined in the lower troposphere (i.e., below  $\sim$ 2.5 km). Furthermore, the maximum aerosol concentrations are frequently found below 2 km. The pronounced aerosol heating rates (1.0 to 3.0 K day<sup>-1</sup>) are correspondingly situated below 2 km, leads to enhanced stability in the lower atmosphere and suppressed convection processes.

#### References:

Aruna, K., Kumar, T. V., Rao, D. N., Murthy, B. V., Babu, S. S., Moorthy, K. K.: Black carbon aerosols in a tropical semi-urban coastal environment: Effects of boundary layer dynamics and long range transport. *J. Atmos. Sol-Terr. Phys.*, 104(5), 116-125, doi: 10.1016/j.jastp.2013.08.020, 2013.

Barbaro, E., Arellano, V. G., Krol, M. C., Holtslag, A. A.: Impacts of aerosol shortwave radiation absorption on the dynamics of an idealized convective atmospheric boundary layer, *Bound-Lay. Meteorol.*, 148(1), 31-49, doi:10.1007/s10546-013-9800-7, 2013.

Cao, J. J., Shen, Z. X., Chow, J. C., Watson, J. G., Lee, S. C., Tie, X. X., Ho, K. F., Wang, G. H., Han, Y. M.: Winter and summer PM2.5 chemical compositions in fourteen Chinese cities, *J. Air. Waste. Manag. Assoc.*, 62(10), 1214-1226,

[Printer-friendly version](#)

[Discussion paper](#)



Ding, A. J., Fu, C. B., Yang, X. Q., Sun, J. N., Peteja, T., Kerminen, V. M., Wang, T., Xie, Y. N., Herrmann, E., Zheng, L. F., Nie, W., Liu, Q., Wei, X. L., and Kulmala, M.: Intense atmospheric pollution modifies weather: a case of mixed biomass burning with fossil fuel combustion pollution in eastern China, *Atmos. Chem. Phys.*, 13, 10545–10554, 20 doi:10.5194/acp-13-10545-2013, 2013.

Interactive comment

Huang, R. J., Zhang, Y., Bozzetti, C., Ho, K. F., Cao, J. J., Han, Y. M., Daellenbach, K. R., Slowik, J. G., Platt, S. M., Canonaco, F., Zotter, P., Wolf, R., Pieber, S. M., Bruns, E. A., Crippa, M., Ciarelli, G., Piazzalunga, A., Schwikowski, M., Abbaszade, G., Schnelle-Kreis, J., Zimmermann, R., An, Z. S., Szidat, S., Baltensperger, U., Haddad I. E., and Prévôt A. S.: High secondary aerosol contribution to particulate pollution during haze events in China, *Nature*, 514, 218–222, doi:10.1038/nature13774, 2014.

Johnson, B. T., Shine, K. P., and Forster, P. M.: The semi-direct aerosol effect: Impact of absorbing aerosols on marine stratocumulus, *Q. J. Roy. Meteorol. Soc.*, 130, 1407–1422, doi: 10.1256/qj.03.61, 2004.

Li, Z. Q., Lee, K. H., Wang, Y. S., Xin, J. Y., Hao, W. M.: First observation-based estimates of cloud-free aerosol radiative forcing across China, *J. Geophys. Res.*, 115, d00k18, doi:10.1029/2009JD013306, 2010.

Sotogarcía, L. L., Andreae, M. O., Andreae, T. W., Artaxo, P., Maenhaut, W., Kirchstetter, T., Novakov, T., Chow, J. C., Mayolbracero, O. L.: Evaluation of the carbon content of aerosols from the burning of biomass in the Brazilian Amazon using thermal, optical and thermal-optical analysis methods, *Atmos. Chem. Phys.*, 11, 4425–4444, doi:10.5194/acp-11-4425-2011, 2011.

Tesfaye, M., Botai, J., Sivakumar, V., Tsidu, G. M.: Simulation of biomass burning aerosols mass distributions and their direct and semi-direct effects over south africa using a regional climate model, *Meteorol. Atmos. Phys.*, 125(3), 177–195,

Printer-friendly version

Discussion paper



Wang, L. L., Xin, J. Y., Li, X. R., Wang, Y. S.: The variability of biomass burning and its influence on regional aerosol properties during the wheat harvest season in North China, *Atmos. Res.*, 157, 153–163, doi: 10.1016/j.atmosres.2015.01.009, 2015.

Wang, Y. Q., Zhang, X. Y., Sun, J. Y., Zhang, X. C., Che, H. Z., and Li, Y.: Spatial and temporal variations of the concentrations of PM10, PM2.5 and PM1 in China, *Atmos. Chem. Phys.*, 15, 13585–13598, doi:10.5194/acp-15-13585-2015, 2015.

Weingartner, E., Saathoff, H., Schnaiter, M., Streit, N., Bitnar, B., Baltensperger, U.: Absorption of light by soot particles: determination of the absorption coefficient by means of aethalometers, *J. Aeros. Sci.*, 34(10), 1445–1463, doi:10.1016/S0021-8502(03)00359-8, 2003.

Xia, X. A., Li, Z. Q., Holben, B., Wang, P. C., Eck, T., Chen, H. B., Cribb, M., Zhao, Y. X.: Aerosol optical properties and radiative effects in the Yangtze Delta region of China, *J. Geophys. Res.*, 112, d22s12, doi:10.1029/2007JD008859, 2007a.

Xia, X. A., Chen, H. B., Li, Z. Q., Wang, P. C., Wang J.: Significant reduction of surface solar irradiance induced by aerosols in a suburban region in northeastern China, *J. Geophys. Res.*, 112, D22S02, doi:10.1029/2006JD007562, 2007b.

Zhang, Y., Fu, R., Yu, H. B., Dickinson, R. E., Juarez, R. N., Chin, M., Wang, H.: A regional climate model study of how biomass burning aerosol impacts land-atmosphere interactions over the Amazon, *J. Geophys. Res.*, 113, d14s15, doi:10.1029/2007jd009449, 2008.

---

Interactive comment on *Atmos. Chem. Phys. Discuss.*, doi:10.5194/acp-2017-2, 2017.

[Printer-friendly version](#)

[Discussion paper](#)



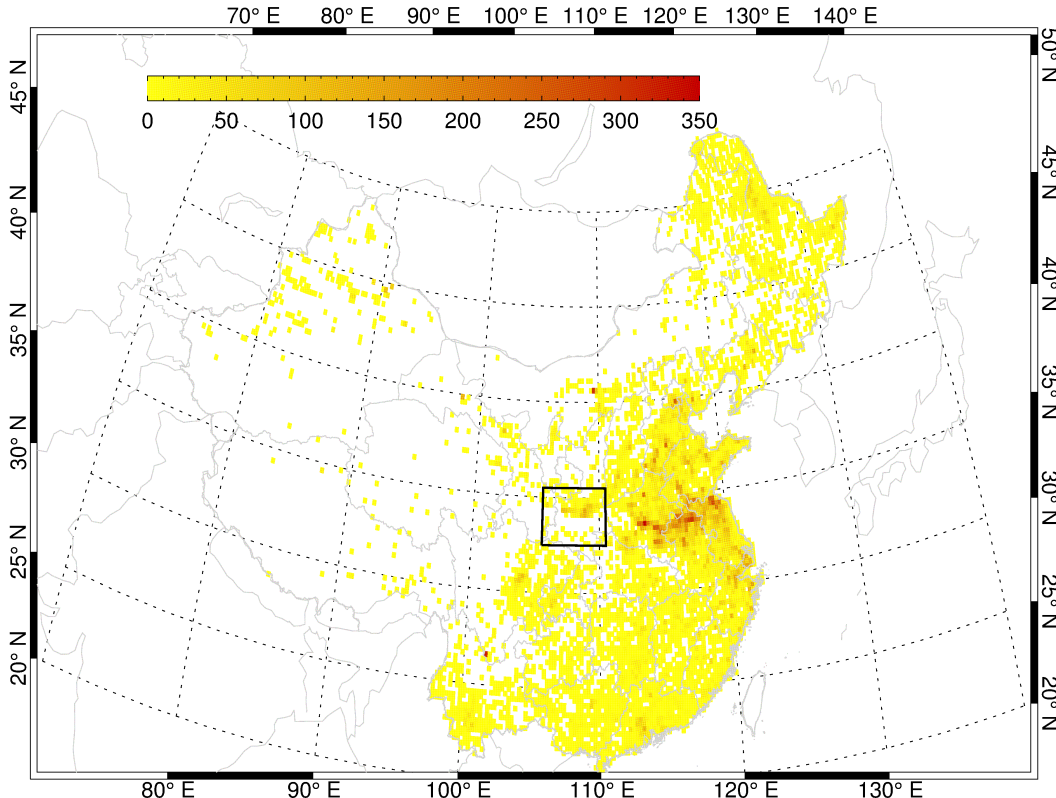


**Fig. 1.** Spatial distribution of daytime fire counts in summer during 2002–2014 over mainland China based on AQUA/MODIS Collection 6 Active Fire Product, the black box shows the study region

[Printer-friendly version](#)

[Discussion paper](#)



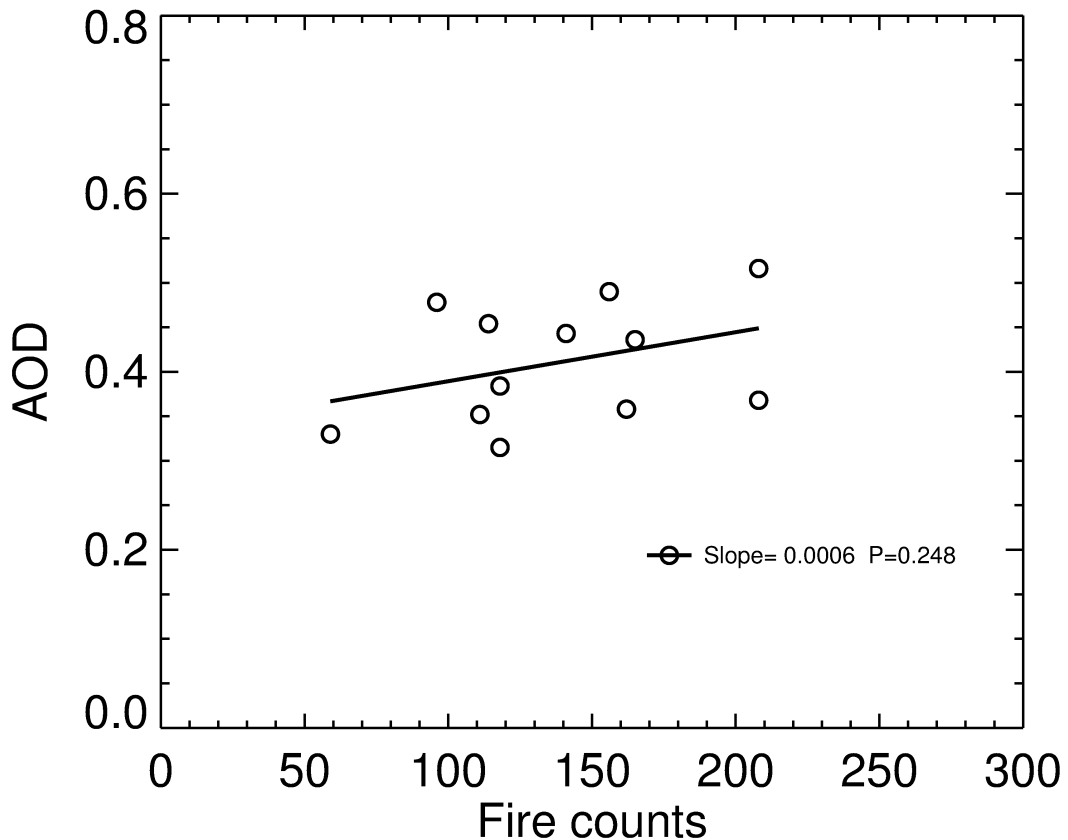


**Fig. 2.** Scatterplots of AOD as a function of the fire counts over Guanzhong plain

[Printer-friendly version](#)

[Discussion paper](#)



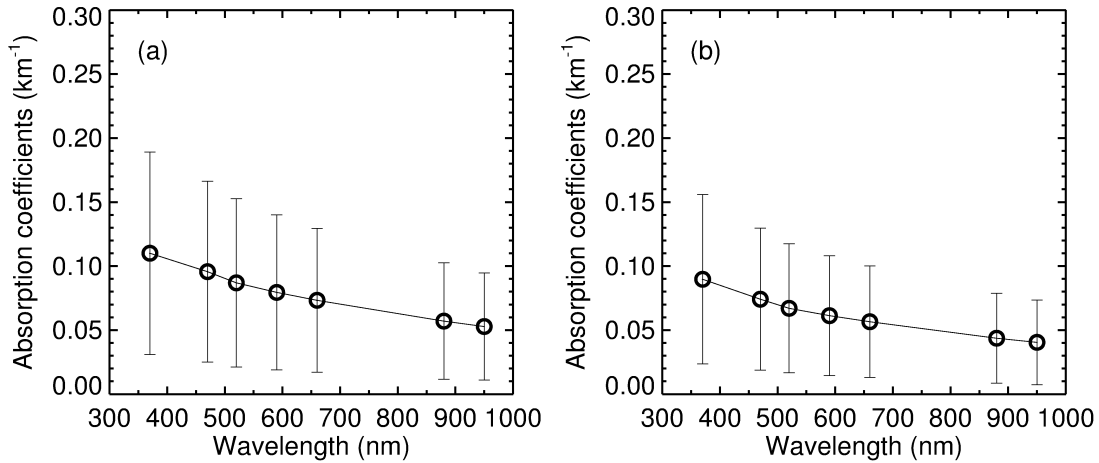


**Fig. 3.** Spectral values of the absorption coefficients measured by Aethalometer (Model AE-31) in summer of (a) 2011 and (b) 2012 at Xi'an

Printer-friendly version

Discussion paper



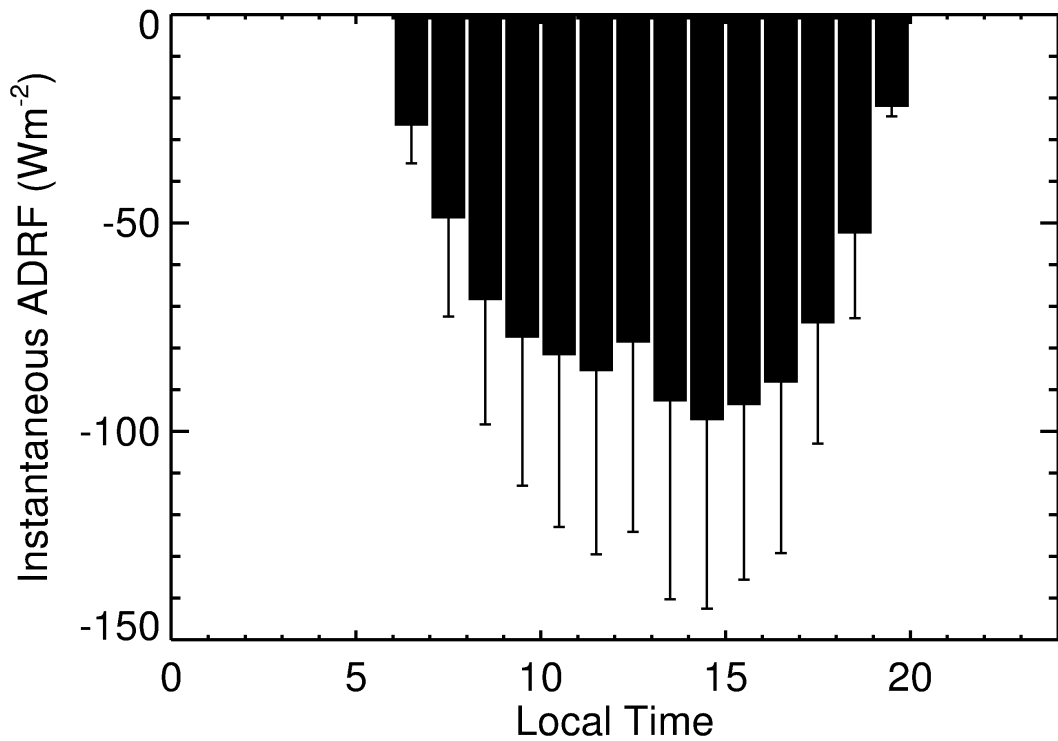


**Fig. 4.** Seasonal mean diurnal variation of the instantaneous ADRF

[Printer-friendly version](#)

[Discussion paper](#)

